



## RESEARCH LETTER

10.1002/2016GL070396

## Key Points:

- ITCZ narrows with global warming in CMIP5 simulations
- Physical mechanisms for ITCZ width changes diagnosed using a theoretical framework
- Opposing ITCZ-width tendencies from enhanced SW heating and meridional moist static energy gradients

## Supporting Information:

- Supporting Information S1

## Correspondence to:

M. P. Byrne,  
byrnem6@tcd.ie

## Citation:

Byrne, M. P., and T. Schneider (2016), Narrowing of the ITCZ in a warming climate: Physical mechanisms, *Geophys. Res. Lett.*, *43*, 11,350–11,357, doi:10.1002/2016GL070396.

Received 11 JUL 2016

Accepted 14 OCT 2016

Accepted article online 22 OCT 2016

Published online 9 NOV 2016

## Narrowing of the ITCZ in a warming climate: Physical mechanisms

Michael P. Byrne<sup>1</sup> and Tapio Schneider<sup>2</sup>

<sup>1</sup>Geological Institute, ETH Zürich, Zürich, Switzerland, <sup>2</sup>Department of Environmental Science and Engineering, California Institute of Technology, Pasadena, California, USA

**Abstract** The Intertropical Convergence Zone (ITCZ) narrows in response to global warming in both observations and climate models. However, a physical understanding of this narrowing is lacking. Here we show that the narrowing of the ITCZ in simulations of future climate is related to changes in the moist static energy (MSE) budget. MSE advection by the mean circulation and MSE divergence by transient eddies tend to narrow the ITCZ, while changes in net energy input to the atmosphere and the gross moist stability tend to widen the ITCZ. The narrowing tendency arises because the meridional MSE gradient strengthens with warming, whereas the largest widening tendency is due to increasing shortwave heating of the atmosphere. The magnitude of the ITCZ narrowing depends strongly on the gross moist stability and clouds, emphasizing the need to better understand these fundamental processes in the tropical atmosphere.

### 1. Introduction

The Intertropical Convergence Zone (ITCZ) is a region of low-level mass convergence and intense rainfall that circles the equatorial Earth. Regional climate in the tropics is strongly affected by the ITCZ, and consequently, it is important to understand the physical processes determining the location, strength, and width of the ITCZ, and how it responds to radiative forcing and natural variability. Considerable research has been devoted to understanding the responses of both the location of the ITCZ [e.g., *Philander et al.*, 1996; *Kang et al.*, 2008; *Schneider et al.*, 2014] and the strength of the vertical motion within the ITCZ [e.g., *Schneider*, 2006; *Vecchi and Soden*, 2007; *Schneider et al.*, 2010; *Bony et al.*, 2013; *Bellomo and Clement*, 2015] to changes in climate. The widening of the Hadley circulation with global warming has also been intensively investigated [e.g., *Lu et al.*, 2007; *Seidel et al.*, 2008; *Waugh et al.*, 2015, 2008; *Levine and Schneider*, 2015]. The response of the ITCZ width to climate change has received little attention in comparison, despite its importance not only for regional precipitation but also for potentially regulating the tropical climate [*Pierrehumbert*, 1995].

Rainfall observations and reanalysis data show a significant narrowing of the Pacific ITCZ over recent decades [*Wodzicki and Rapp*, 2016]. The ITCZ also narrows in global climate model (GCM) simulations of future warming [*Huang et al.*, 2013; *Lau and Kim*, 2015]. It has been speculated that the narrowing of the ITCZ is related to upper tropospheric relative humidity and cloud-radiative feedbacks [*Lau and Kim*, 2015], but a complete mechanistic understanding is lacking. The ITCZ width (or, more generally, the ratio of the areas of upward motion to downward motion in the tropics) has been found to depend on different physical processes in a variety of analytical and idealized models, including the gross moist stability (GMS) [*Bretherton and Sobel*, 2002], the horizontal diffusivity of moisture [*Sobel and Neelin*, 2006], cloud-radiative and water vapor-radiative effects [*Bretherton and Sobel*, 2002; *Voigt and Shaw*, 2015; *Harrop and Hartmann*, 2016], and the skewness of the vertical velocity distribution [*Pendergrass and Gerber*, 2016]. The “upped-ante mechanism” [*Neelin et al.*, 2003] explains a reduction in precipitation on the margins of tropical convective regions and is associated with changes in horizontal moisture advection. However, the extent to which these processes control the ITCZ width in comprehensive climate models has not been established nor is it clear which processes are responsible for the narrowing of the ITCZ with warming.

To understand why the ITCZ narrows as the climate warms, we use the theoretical framework developed by *Byrne and Schneider* [2016], which permits a mechanistic decomposition of the processes contributing to changes in ITCZ width. *Byrne and Schneider* [2016] derived a diagnostic scaling for the ITCZ width using the mass and energy budgets of the atmosphere and applied the scaling to idealized GCM simulations over a wide range of climates. The ITCZ width was found to depend on four physical factors: net energy input to the

tropical atmosphere, advection of moist static energy (MSE) by the mean flow, divergence of MSE by transient eddies, and the GMS (the GMS characterizes the efficiency per unit mass transport with which divergent circulations import or export energy). Some of these factors have been previously identified as influencing the ITCZ width, but the *Byrne and Schneider* [2016] framework allows changes in these processes to be explicitly and quantitatively linked to changes in ITCZ width. This helps elucidate the physical mechanisms responsible for the changes.

Here we analyze changes in ITCZ width in more realistic models from the Coupled Model Intercomparison Project Phase 5 (CMIP5) [*Taylor et al.*, 2012] in order to better understand how and why the ITCZ width changes with global warming. We begin by examining the simulated changes in ITCZ width (section 2) before discussing the physical processes responsible for these changes (section 3). We conclude with a summary and discussion of our results and an outlook for future research (section 4).

## 2. ITCZ Width Changes in CMIP5 Models

### 2.1. Definition of ITCZ Width

Following *Byrne and Schneider* [2016], we define the zonal-mean ITCZ as the band of tropical latitudes where there is time-mean low-level mass convergence or, equivalently, where there is upward motion (see Figure 2 of *Byrne and Schneider* [2016] for a visualization of this definition). The ITCZ width is the meridional distance between the northern and southern edges of this region of upward motion. We compute the ITCZ width using the middle-tropospheric mass stream function  $\Psi$ . Vertical velocity is proportional to the meridional gradient of the mass stream function, i.e.,  $\omega \propto -\partial\Psi/\partial\phi$ , where  $\omega$  is the vertical (pressure) velocity and  $\phi$  is latitude. The ITCZ width is calculated as the distance between the maxima in absolute mass stream function, where  $\partial\Psi/\partial\phi = 0$ , north and south of the equator. The ITCZ width, calculated using this method and data from the ERA-Interim reanalysis [*Dee et al.*, 2011] averaged between 1998 and 2014, is  $27^\circ$  of latitude [*Byrne and Schneider*, 2016]. The ITCZ at certain longitudes, particularly over the Atlantic and Pacific Oceans, is substantially narrower than  $27^\circ$  [see *Byrne and Schneider*, 2016, Figure 1]. However, the ITCZ is wide in the zonal mean because (a) the meridional position varies zonally and (b) the ITCZ in the annual mean is quite broad in some regions with large seasonal variability (e.g., South Asian monsoon). Denoting the northern and southern edges of the zonal-mean ITCZ as  $\phi_{i,N}$  and  $\phi_{i,S}$ , respectively, the area of the ITCZ is  $A_i = 2\pi R^2(\sin\phi_{i,N} - \sin\phi_{i,S})$ , where  $R$  is Earth's radius. The descent area,  $A_d$ , which we will also discuss, is the portion of the Hadley circulation where there is time-mean descending motion. The descent area is calculated as the total area of the Hadley circulation minus the ITCZ area, where, following *Lu et al.* [2007], the edges of the Hadley circulation are identified as the subtropical latitudes where the middle-tropospheric mass stream function passes through zero.

### 2.2. Simulated Changes

We calculate the ITCZ area in the historical (1976–2005) and RCP8.5 (2070–2099) simulations for 20 CMIP5 models (see Text S1 in the supporting information for a list of the models analyzed). Changes in ITCZ area  $\delta A_i$  are defined as the area in RCP8.5 minus the area in the historical simulation. To calculate the ITCZ area, we first compute the Eulerian-mean mass stream function using annual-mean meridional velocities [e.g., *Peixoto and Oort*, 1984]. The stream function is averaged vertically (with mass weighting) between 700 hPa and 300 hPa, and the ITCZ and Hadley circulation edges are identified as the latitudes where the averaged stream function has a local maximum or passes through zero, respectively. The multimodel-mean ratio of the ITCZ area to the total area of the Hadley circulation is 46% in the CMIP5 historical simulations: Approximately half of the annual-mean simulated Hadley circulation has time-mean upward motion (this ratio is 48% in December–February (DJF) and 41% in June–August (JJA) and is likely to vary zonally).

More than three quarters of models analyzed (16 out of 20) show a narrowing of the ITCZ as the climate warms (Figure 1). The multimodel-mean narrowing of the ITCZ per unit global warming is  $0.7\% \text{ K}^{-1}$  (with an interquartile range of  $1.5\% \text{ K}^{-1}$ ), which is similar in magnitude to the projected widening of the Hadley circulation with warming ( $0.8\% \text{ K}^{-1}$  in these simulations); it is small relative to the fractional increase in the descent area ( $2.1\% \text{ K}^{-1}$ ; Figure 1). The narrowing of the ITCZ and the widening of the Hadley circulation both contribute to the projected expansion of the dry descent region under global warming, with the contribution from the widening of the Hadley circulation typically larger in magnitude. Interestingly, there is a strong anticorrelation between fractional changes in the ITCZ and descent areas ( $r = -0.88$ ): As the dry descent region widens

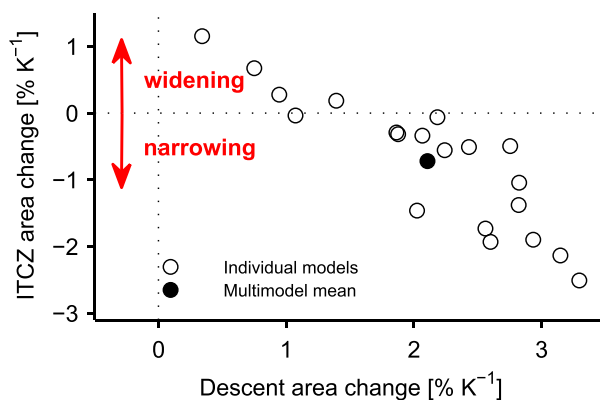


**Figure 1.** Fractional changes in ITCZ area versus fractional changes in descent area for individual CMIP5 models (open black circles) and for the multimodel mean (solid black circle). The fractional area changes are normalized by the global-mean surface-air temperature change for each model. Here and for all subsequent figures, changes are calculated between the historical (1976–2005) and RCP8.5 (2070–2099) simulations.

consistent with a northward shift of the ITCZ edge. At the northern edge of the ITCZ, the change in vertical velocity is close to zero, and there is little change in the latitude of the northern edge of the ITCZ. The majority of models show a northward shift of the southern edge of the ITCZ with global warming (multimodel-mean shift of +0.8°; Figure S1); there is no clear shift in the northern edge of the ITCZ, with approximately half the models moving it northward and the other half moving it southward (multimodel-mean shift of +0.1°; Figure S1). These shifts in the edges of the ITCZ, with the southern edge moving northward and the northern edge remaining roughly at the same latitude, are consistent with an overall narrowing of the ITCZ with global warming. Observed trends in the locations of the edges of the Pacific ITCZ also show this north-south asymmetry, with the southern edge having migrated farther northward than the northern edge has migrated southward over recent decades [Wodzicki and Rapp, 2016].

It is possible that the annual-mean narrowing of the ITCZ as the climate warms could result from a reduced seasonal migration of the ITCZ in a warmer climate. However, the seasonal migration of the ITCZ (defined as the area between the average JJA and DJF locations of the ITCZ) increases with warming in the majority of models (Figure S2), is only very weakly correlated with annual-mean ITCZ width changes, and thus does not

explain the annual-mean narrowing of the ITCZ with warming.

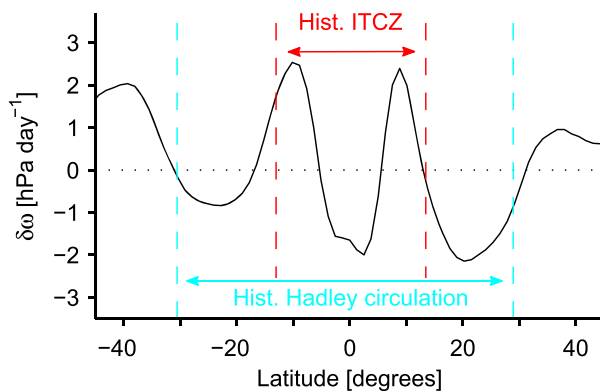


**Figure 2.** The zonal-, annual-, and multimodel-mean change in vertical velocity averaged between 300 hPa and 700 hPa (solid black line). Dashed red lines denote the multimodel-mean edges of the historical ITCZ as defined using the mass stream function technique, and dashed blue lines show the edges of the historical Hadley circulation (defined as the subtropical latitudes at which the mass stream function passes through zero).

with warming, the wet ITCZ tends to narrow. A similar anticorrelation between changes in the areas of the ITCZ and descent region is also found in idealized GCM simulations over a wide range of climates [Byrne and Schneider, 2016].

The narrowing of the ITCZ as the climate warms is evident in zonal-mean vertical velocity changes (Figure 2). Upward motion is strengthened at the center of the ITCZ, close to the equator, but diminished on the equatorward margins of the ITCZ (this is the “deep-tropics squeeze” described by Lau and Kim [2015]). Downward motion in the descent region generally weakens as the climate warms (Figure 2), consistent with a slowdown of the tropical overturning circulation [e.g., Lu et al., 2007]. At the southern edge of the ITCZ, the change in downward motion is

### 2.3. Mass ITCZ Versus Moisture ITCZ

The ITCZ is commonly associated with intense rainfall, and so it is instructive to compare the low-level mass-convergence definition of the ITCZ described above (the “mass ITCZ”) with a hydrological definition of the ITCZ. In analogy to the poleward extent of subtropical dry zones, which is often defined as the subtropical latitude where zonal-mean precipitation minus evaporation ( $P - E$ ) passes through zero [e.g., Lu et al., 2007], an alternative definition of the ITCZ is the equatorial region where there is time-mean atmospheric moisture convergence, i.e., where  $P - E > 0$ . This definition has been applied to idealized simulations of climate change and is termed the “moisture

ITCZ" [Byrne and Schneider, 2016]. If atmospheric moisture convergence in the tropics is associated solely with the mean divergent flow (see equation (A1) in Appendix A), then the mass and moisture ITCZs will coincide. However, if moisture divergence by transient eddies or advection of moisture by the mean flow are non-negligible in the tropics, the widths of the mass and moisture ITCZs will not generally be equal (as is the case in the idealized simulations of Byrne and Schneider [2016]). In the CMIP5 historical simulations, the multimodel-mean mass ITCZ is wider than the moisture ITCZ by approximately  $5^\circ$  of latitude (Figure S3). This is consistent with transient eddies and mean advection exerting a substantial drying influence on the tropical atmosphere (Figure S4a). Fractional changes in the areas of the mass and moisture ITCZs are reasonably well correlated ( $r=0.54$ ; Figure S5) and very well correlated ( $r=0.75$ ) when one model which shows highly anomalous changes in moisture convergence is excluded from the analysis. Thus, inferences about changes in the mass ITCZ will largely carry over to the moisture ITCZ. In the next section, we examine the physical processes controlling the width of the mass ITCZ.

### 3. Physical Mechanisms

#### 3.1. Application of Diagnostic Scaling

To understand why climate models mostly show a narrowing of the ITCZ with warming, we apply a diagnostic scaling for the ITCZ width based on the mass and energy budgets of the atmosphere [Byrne and Schneider, 2016]. The scaling relates fractional changes in ITCZ area, relative to fractional changes in the descent area, to changes in atmospheric, oceanic, and radiative processes (for a derivation see Appendix B and section 3 of Byrne and Schneider [2016]):

$$\frac{\delta A_i}{A_i} - \frac{\delta A_d}{A_d} = \underbrace{\frac{\delta(\Delta h_i)}{\Delta h_i} - \frac{\delta(\Delta h_d)}{\Delta h_d}}_{\delta\text{GMS}} + \frac{1}{H_i} \left[ \delta\langle \bar{S} - \bar{L} - \bar{O} \rangle_d \frac{H_i}{H_d} - \delta\langle \bar{S} - \bar{L} - \bar{O} \rangle_i \right]_{\delta\text{NEI}} - \underbrace{\frac{1}{H_i} \left[ \delta\langle \{\bar{v} \cdot \nabla \bar{h}\} \rangle_d \frac{H_i}{H_d} - \delta\langle \{\bar{v} \cdot \nabla \bar{h}\} \rangle_i \right]}_{\delta\text{MeanAdv}} - \underbrace{\frac{1}{H_i} \left[ \delta\langle \{\nabla \cdot \bar{v}'h'\} \rangle_d \frac{H_i}{H_d} - \delta\langle \{\nabla \cdot \bar{v}'h'\} \rangle_i \right]}_{\delta\text{Eddy}}. \quad (1)$$

In the equation above  $\Delta h$  is the GMS, similar to that defined by Neelin and Held [1987],  $S$  is the net downward top-of-atmosphere (TOA) shortwave radiative flux,  $L$  is the net upward TOA longwave radiative flux,  $O$  is the ocean heat uptake,  $v$  is the meridional wind, and  $h$  is the MSE per unit mass.  $H = \langle \{\bar{h}(\nabla \cdot \bar{v})\} \rangle = -\Delta h \bar{\omega}$  is the vertically integrated MSE divergence associated with the divergent mean flow, where  $\bar{\omega}$  is a bulk vertical velocity averaged over either the ITCZ or the descent region (see Appendix B). The subscripts  $i$  and  $d$  denote quantities that are spatially averaged over either the ITCZ or the descent region in the historical simulations, respectively,  $\langle \cdot \rangle_i$  and  $\langle \cdot \rangle_d$  are the spatial-averaging operators, overlines denote climatological monthly means, and primes denote departures from monthly means. The net energy input per unit area to the atmosphere is  $\bar{S} - \bar{L} - \bar{O}$ . The operator  $\{ \cdot \}$  indicates a mass-weighted vertical integral over the atmosphere. The scaling relates fractional changes in ITCZ area  $\delta A_i/A_i$ , relative to fractional changes in the descent area  $\delta A_d/A_d$ , to changes in GMS ( $\delta\text{GMS}$ ), net energy input to the atmosphere ( $\delta\text{NEI}$ ), the mean meridional advection of MSE ( $\delta\text{MeanAdv}$ ), and the transient-eddy MSE divergence ( $\delta\text{Eddy}$ ).

We apply the diagnostic scaling (1) to elucidate the physical processes responsible for ITCZ width changes under global warming in CMIP5 simulations (a detailed description of how the scaling is applied to these simulations is provided in Appendix B). The scaling captures the simulated ITCZ changes (Figure 3), confirming that it is a useful tool for understanding how and why the ITCZ changes with climate. The ITCZ narrows relative to the descent region in all but one of the models analyzed (Figure 3), with a multimodel-mean simulated narrowing of  $2.8 \text{ K}^{-1}$  compared to an estimate from the scaling of  $2.9 \text{ K}^{-1}$ .

#### 3.2. Interpretation of Narrowing and Widening Tendencies

As the climate warms, different physical processes influence the ITCZ width in opposing ways. In particular, multimodel-mean changes in GMS ( $+7.7\% \text{ K}^{-1}$ ) and net energy input ( $+12.3\% \text{ K}^{-1}$ ) tend to widen the ITCZ with warming, whereas changes in the mean advection of MSE ( $-14.6\% \text{ K}^{-1}$ ) and in transient-eddy MSE divergence ( $-8.4\% \text{ K}^{-1}$ ) tend to narrow the ITCZ (Figure 3). Each component of the diagnostic scaling contains two contributions: one due to changes in the ITCZ (subscript  $i$ ) and another due to changes in the descent region (subscript  $d$ ). Processes in the descent region generally have a smaller influence on fractional changes in ITCZ

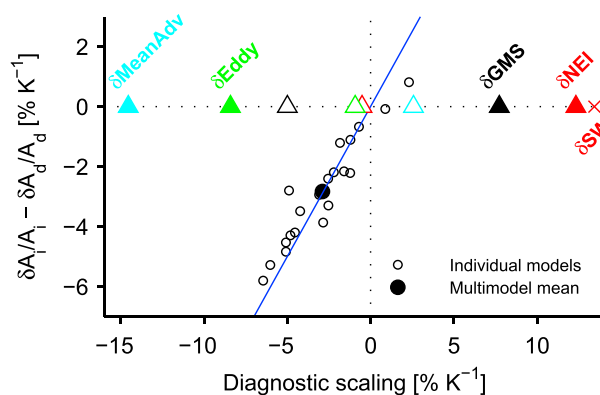


**Figure 3.** Scatterplot of fractional changes in ITCZ area relative to fractional changes in descent area vs estimates from the diagnostic scaling (1) for each model (open black circles,  $r=0.95$ ) and for the multimodel mean (solid black circle). The multimodel-mean components of the scaling are also shown (solid triangles of various colors) along with the shortwave component of the net energy input term:  $\delta SW = (1/H_i) [\delta \langle \bar{S} \rangle_d (H_i/H_d) - \delta \langle \bar{S} \rangle_i]$  (red cross). The contributions to each component from changes in the descent region only are also plotted (open triangles with the colors corresponding to those of the solid triangles for each component), as is the one-to-one relationship (blue line).

which show a greater sensitivity of ITCZ width to changes in the descent region [Byrne and Schneider, 2016] because  $|H_i| > |H_d|$  in those simulations.

The influence of changes in the atmospheric energy budget under global warming on the ITCZ width can be understood physically by considering the energy budget in conjunction with the mass budget of the Hadley circulation. Why does the  $\delta NEI$  component have a widening influence on the ITCZ? The net energy input to the ITCZ increases with warming in all models (Figure S6a), and it increases more strongly in the ITCZ than at higher latitudes (cf. Figures S6a and S6b), consistent with an enhanced poleward flux of MSE by the atmosphere. Most models analyzed here have a small and negative mean-divergent component of the atmospheric energy budget in the ITCZ (see, for example, the IPSL-CM5A-LR model; Figure S4b), implying that the mean divergent circulation is importing MSE to the ITCZ in the zonal mean and that the GMS is negative. Therefore, to energetically balance the differential increase in net energy input to the ITCZ, the divergent (vertical) mass flux in the ITCZ must decrease, for fixed GMS. From the Hadley-circulation mass budget (B3), a decrease in the vertical mass flux in the ITCZ implies a widening of the ITCZ. The increase in net energy input to the ITCZ is due mostly to an increase in shortwave heating (cf. the solid red triangle and the red cross; Figure 3), with changes in longwave cooling and ocean heat uptake having a negligible influence on the ITCZ width by comparison (not shown).

Decomposing the influence of an increase in net energy input on the ITCZ width into all-sky (including cloud-radiative effects) and clear-sky (excluding cloud-radiative effects) parts, changes in clear-sky radiative fluxes are found to give a multimodel-mean ITCZ widening tendency of  $3.4\% K^{-1}$ . This compares to an overall widening tendency of  $11.2\% K^{-1}$  when cloud-radiative effects are included (this analysis is performed on a subset of 16 models, listed in Text S1 in the supporting information, for which the clear-sky radiative fluxes were available). Thus, there is a close coupling between clouds and the tropical circulation (as highlighted previously [e.g., Bony et al., 2015]), with changes in shortwave radiative fluxes associated with clouds tending to widen the ITCZ substantially (by  $7.8\% K^{-1}$ ). Increased clear-sky absorption of shortwave radiation due to a moistening of the atmosphere as the climate warms is an expected consequence of global warming [e.g., DeAngelis et al., 2015]. The reason for the strong increase in shortwave heating in the ITCZ due to changes in clouds is less clear, though it is likely related to a reduction of approximately 1% in the total cloud fraction in the ITCZ as the climate warms (not shown) and potentially to changes in the vertical distribution of tropical clouds.

width (relative to fractional changes in descent area) than changes in the ITCZ itself (cf. the open and solid triangles; Figure 3). For the  $\delta NEI$ ,  $\delta MeanAdv$ , and  $\delta Eddy$  terms, the reason for the large sensitivity to changes in the ITCZ is that the magnitude of the mean divergent component of the atmospheric energy budget is smaller in the ITCZ than in the descent region; i.e.,  $|H_i| < |H_d|$  (Figure S4b). This means that for a given perturbation to the atmospheric energy budget per unit area (due to a reduction in outgoing longwave radiation, say) a larger fractional change in vertical velocity is needed in the ITCZ than in the descent region for energetic balance to be reestablished (assuming fixed GMS). This result follows from a straight forward analysis of the atmospheric energy budget (B1) and implies, via the Hadley circulation mass budget (B3), that processes in the ITCZ have a dominant influence on changes in ITCZ width. However, the opposite is the case in idealized GCM simulations

Analogous arguments can be made for the impacts of changes in mean meridional MSE advection of MSE, transient-eddy MSE divergence, and GMS on the ITCZ width. Cooling of the ITCZ by mean meridional MSE advection and transient-eddy MSE divergence increases under global warming (Figure S6a). This enhanced cooling of the ITCZ results from steeper meridional MSE gradients at low latitudes in a warmer climate (Figure S7), primarily because of differentially increased specific humidity, meaning that the atmosphere exports more energy from the tropics via mean advection and transient eddies even if the circulation strength does not change. To balance this increased cooling of the ITCZ, the upward mass flux in the ITCZ must increase (for negative GMS), implying a narrowing of the ITCZ relative to the descent region. Changes in GMS in the ITCZ and the descent region have opposing effects on ITCZ width. In the ITCZ, the GMS decreases with warming in most models (i.e., GMS becomes more negative as the climate warms), implying reduced ascent in the ITCZ (in order to import the same quantity of MSE) and a widening tendency. In the descent region, the GMS increases with warming in all models (i.e., becomes more positive in qualitative agreement with simple thermodynamic scalings [Held, 2001; Hill *et al.*, 2015]) which requires reduced descent for energetic balance and is thus a narrowing tendency for the ITCZ.

The influence of changes in net energy input and other processes on the ITCZ width depend nonlinearly on the control-climate GMS in the ITCZ. In particular, the magnitude of the widening or narrowing tendency is inversely proportional to the magnitude of the GMS. Most models analyzed here have a negative GMS in the ITCZ (Figure S8) meaning that increases in net energy input tend to narrow the ITCZ. However, for models with positive GMS (4 of the 20 models analyzed here), increases in net energy input widen the ITCZ. Indeed, of the four models that simulate an increase in ITCZ width with warming, two have positive GMS in the ITCZ. This sensitive dependence of ITCZ width on GMS emphasizes the need to better understand the physics determining the tropical GMS and the differences in simulated GMS across models (Figure S8).

#### 4. Discussion

In contrast to the observed and projected widening of the Hadley circulation, the ITCZ narrows as the climate warms. Models predict an ITCZ narrowing of  $0.7\% \text{ K}^{-1}$  relative to the historical period, which is comparable (in a fractional sense) to the widening of the Hadley circulation ( $0.8\% \text{ K}^{-1}$ ). The narrowing of the ITCZ is likely to affect regional climates and societies on the margins of the ITCZ and may also have important implications for global climate through its effect on the planetary radiative balance [Pierrehumbert, 1995; Bony *et al.*, 2016].

Changes in the ITCZ width defined using low-level mass convergence (the mass ITCZ) are well correlated with changes in a hydrological measure of the ITCZ (the moisture ITCZ), indicating that a narrowing of the ascending branch of the Hadley circulation will likely be associated with a narrowing of the area of tropical moisture convergence and substantial changes in the regional water cycle. We find the ITCZ narrowing to be predominantly due to a northward shift of the southern edge of the ITCZ, though the reasons for this hemispherically asymmetric response remain to be determined.

Using a theoretical framework derived by Byrne and Schneider [2016], we analyzed the processes responsible for the narrowing of the ITCZ with warming. The narrowing tendency is due largely to an enhanced meridional MSE gradient in a warmer climate, which increases cooling of the ITCZ by both transient eddies and the advective component of the Hadley circulation. Increased atmospheric moisture content in a warmer climate is responsible for the steepening of the MSE gradient and thus for the ITCZ narrowing tendency. The narrowing of the ITCZ is partly opposed by other climate processes which tend to widen the ITCZ, namely, an increase in the net energy input to the ITCZ (dominated by an increase in shortwave heating due to both cloud and clear-sky effects) and changes in the GMS. How the width of the ITCZ changes with climate depends strongly on the control-climate GMS in the ITCZ. This analysis and physical interpretation of why the ITCZ narrows with warming represents a fundamental advance in our understanding of the atmospheric general circulation and how it responds to radiative forcing.

We are only beginning to understand the structure of the ITCZ and its sensitivity to changes in climate and many outstanding questions remain. In particular, how is the narrowing of the ITCZ manifested over the seasonal cycle, and does it have implications for monsoon dynamics? Why do the northern and southern edges of the ITCZ respond differently to global warming? How does the width of the ITCZ change as a function of longitude? Are changes in ITCZ width an important feedback on global climate change? Finally, can the framework discussed here help to understand the observed narrowing of the ITCZ over recent decades, the evolution of the ITCZ over the course of the seasonal cycle, or the ITCZ response to interannual variability,

for example, the widening associated with El Niño events [Wodzicki and Rapp, 2016]? These questions will form the basis of future work.

## Appendix A: Atmospheric Moisture Budget

The steady state zonal-mean atmospheric moisture budget can be written as [e.g., Byrne and O’Gorman, 2015]

$$P - E = \overbrace{\underbrace{-\{\bar{q}\nabla \cdot \bar{v}\}}_{\text{Mean conv. comp.}} - \underbrace{\{\bar{v} \cdot \nabla \bar{q}\}}_{\text{Mean adv. comp.}} - \underbrace{\{\nabla \cdot \bar{v}'q'\}}_{\text{Transient-eddy conv. comp.}}}_{\text{Total moisture convergence}}, \quad (\text{A1})$$

where  $q$  is the specific humidity and the other quantities and symbols are as defined in the text.

## Appendix B: Evaluation of the Diagnostic Scaling for Changes in ITCZ Width

To evaluate the various terms in the diagnostic scaling (1), we begin with the steady state zonal-mean atmospheric energy budget averaged over a specified latitudinal band [Byrne and Schneider, 2016]:

$$\underbrace{\langle \bar{S} - \bar{L} - \bar{O} \rangle}_{\text{Net energy input}} = \overbrace{\underbrace{-\Delta h \bar{\omega}}_{\text{Mean div. comp.}} + \underbrace{\langle \{\bar{v} \cdot \nabla \bar{h}\} \rangle}_{\text{Mean adv. comp.}} + \underbrace{\langle \nabla \cdot \{\bar{v}'h'\} \rangle}_{\text{Transient-eddy div. comp.}}}_{\text{Total MSE divergence}}, \quad (\text{B1})$$

where  $\bar{\omega}$  is a bulk vertical velocity and the other quantities and symbols are as defined in the text. We have written the total atmospheric MSE divergence (the right-hand side of (B1)) as a function of three terms: a mean divergent component, a mean advection component, and a transient-eddy component. The mean divergent component has been written as a function of the GMS and vertical velocity, following Neelin and Held [1987] (though here we use a bulk vertical velocity, averaged over a specified area). The bulk vertical velocities for the ITCZ and the descent region are respectively:

$$\bar{\omega}_i = \frac{\Psi(\phi_{i,S}) - \Psi(\phi_{i,N})}{A_i}; \quad \bar{\omega}_d = \frac{\Psi(\phi_{i,N}) - \Psi(\phi_{i,S})}{A_d}, \quad (\text{B2})$$

where  $\Psi$  is the mass stream function averaged vertically between 700 hPa and 300 hPa.

The net energy input along with the mean divergent and mean advection components of (B1) are calculated explicitly using the monthly-mean radiative fluxes, surface latent and sensible heat fluxes, specific humidities, temperatures, geopotentials, and horizontal winds outputted by each model. We calculate the mean divergent component as  $H = \{\bar{h}(\nabla \cdot \bar{v})\}$  then divide this by  $-\bar{\omega}$  in order to estimate the GMS in each region:  $\Delta h = -H/\bar{\omega}$ . The transient-eddy divergence is calculated as a residual from the atmospheric energy budget. To assess whether calculating the eddy term as a residual is reasonable, we estimate the eddy term explicitly for one model (IPSL-CM5A-LR) in the historical simulation using daily-mean data (cf. the solid and dashed green lines; Figure S4b). The eddy term calculated explicitly is similar to that estimated as a residual, though the residual technique underestimates the MSE divergence which is likely to be partly due to an under-sampling of the eddy transport by using daily mean, rather than higher-frequency, fields for the explicit calculation. Nevertheless, the use of the residual technique for calculating the transient-eddy divergence is reasonable.

To derive the diagnostic scaling (1), we combine the atmospheric energy budget (B1) with the mass budget of the Hadley circulation. The latter budget is expressed as

$$A_i \bar{\omega}_i = -A_d \bar{\omega}_d. \quad (\text{B3})$$

Combining the mass budget (B3) with the energy budget (B1) averaged over the ITCZ and the descent region separately, we can write the area of the ITCZ, as a fraction of the descent-region area, in terms of other quantities:

$$\frac{A_i}{A_d} = -\frac{\bar{\omega}_d}{\bar{\omega}_i} = -\frac{\langle \bar{S} - \bar{L} - \bar{O} - \{\bar{v} \cdot \nabla \bar{h}\} - \{\nabla \cdot \bar{v}'h'\} \rangle_d \Delta h_i}{\langle \bar{S} - \bar{L} - \bar{O} - \{\bar{v} \cdot \nabla \bar{h}\} - \{\nabla \cdot \bar{v}'h'\} \rangle_i \Delta h_d}. \quad (\text{B4})$$

Linearizing (B4), we recover the diagnostic scaling (1). We note that the diagnostic scaling gives qualitatively similar results when the descent region is defined to be the total area of the Earth outside the ITCZ rather than the portion of the Hadley circulation with time-mean downward motion.

#### Acknowledgments

We thank Paulo Ceppi, Angie Pendergrass, and Robert Wills for helpful discussions. We also thank two anonymous reviewers for their comments and suggestions.

#### References

- Bellomo, K., and A. C. Clement (2015), Evidence for weakening of the Walker circulation from cloud observations, *Geophys. Res. Lett.*, *42*, 7758–7766, doi:10.1002/2015GL065463.
- Bony, S., G. Bellon, D. Kloke, S. Sherwood, S. Fermepein, and S. Denvil (2013), Robust direct effect of carbon dioxide on tropical circulation and regional precipitation, *Nat. Geosci.*, *6*, 447–451.
- Bony, S., et al. (2015), Clouds, circulation and climate sensitivity, *Nat. Geosci.*, *8*, 261–268.
- Bony, S., B. Stevens, D. Coppin, T. Becker, K. A. Reed, A. Voigt, and B. Medeiros (2016), Thermodynamic control of anvil cloud amount, *Proc. Natl. Acad. Sci. U.S.A.*, *113*, 8927–8932.
- Bretherton, C. S., and A. H. Sobel (2002), A simple model of a convectively coupled Walker circulation using the weak temperature gradient approximation, *J. Clim.*, *15*, 2907–2920.
- Byrne, M. P., and P. A. O’Gorman (2015), The response of precipitation minus evapotranspiration to climate warming: Why the “wet-get-wetter, dry-get-drier” scaling does not hold over land, *J. Clim.*, *28*, 8078–8092.
- Byrne, M. P., and T. Schneider (2016), Energetic constraints on the width of the intertropical convergence zone, *J. Clim.*, *29*, 4709–4721.
- DeAngelis, A. M., X. Qu, M. D. Zelinka, and A. Hall (2015), An observational radiative constraint on hydrologic cycle intensification, *Nature*, *528*, 249–253.
- Dee, D. P., et al. (2011), The ERA-Interim reanalysis: Configuration and performance of the data assimilation system, *Q. J. R. Meteorol. Soc.*, *137*, 55–597.
- Harrop, B. E., and D. L. Hartmann (2016), The role of cloud radiative heating in determining the location of the ITCZ in aquaplanet simulations, *J. Clim.*, *29*, 2741–2763.
- Held, I. M. (2001), The partitioning of the poleward energy transport between the tropical ocean and atmosphere, *J. Atmos. Sci.*, *58*, 943–948.
- Hill, S. A., Y. Ming, and I. M. Held (2015), Mechanisms of forced tropical meridional energy flux change, *J. Clim.*, *28*, 1725–1742.
- Huang, P., S.-P. Xie, K. Hu, G. Huang, and R. Huang (2013), Patterns of the seasonal response of tropical rainfall to global warming, *Nat. Geosci.*, *6*, 357–361.
- Kang, S. M., I. M. Held, D. M. W. Frierson, and M. Zhao (2008), The response of the ITCZ to extratropical thermal forcing: Idealized slab-ocean experiments with a GCM, *J. Clim.*, *21*, 3521–3532.
- Lau, W. K. M., and K.-M. Kim (2015), Robust Hadley circulation changes and increasing global dryness due to CO<sub>2</sub> warming from CMIP5 model projections, *Proc. Natl. Acad. Sci. U.S.A.*, *112*, 3630–3635.
- Levine, X. J., and T. Schneider (2015), Baroclinic eddies and the extent of the Hadley circulation: An idealized GCM study, *J. Atmos. Sci.*, *72*, 2744–2761.
- Lu, J., G. A. Vecchi, and T. Reichler (2007), Expansion of the Hadley cell under global warming, *Geophys. Res. Lett.*, *34*, L06805, doi:10.1029/2006GL028443.
- Neelin, J. D., and I. M. Held (1987), Modeling tropical convergence based on the moist static energy budget, *Mon. Weather Rev.*, *115*, 3–12.
- Neelin, J. D., C. Chou, and H. Su (2003), Tropical drought regions in global warming and El Niño teleconnections, *Geophys. Res. Lett.*, *30*(24), 2275, doi:10.1029/2003GL018625.
- Peixoto, J. P., and A. H. Oort (1984), Physics of climate, *Rev. Mod. Phys.*, *56*, 365–429.
- Pendergrass, A. G., and E. P. Gerber (2016), The rain is askew: Two idealized models relating vertical velocity and precipitation distributions in a warming world, *J. Clim.*, *29*, 6445–6462.
- Philander, S. G. H., D. Gu, G. Lambert, T. Li, D. Halpern, N. C. Lau, and R. C. Pacanowski (1996), Why the ITCZ is mostly north of the equator, *J. Clim.*, *9*, 2958–2972.
- Pierrehumbert, R. T. (1995), Thermostats, radiator fins, and the local runaway greenhouse, *J. Atmos. Sci.*, *52*, 1784–1806.
- Schneider, T. (2006), The general circulation of the atmosphere, *Annu. Rev. Earth Planet. Sci.*, *34*, 655–688.
- Schneider, T., P. A. O’Gorman, and X. J. Levine (2010), Water vapor and the dynamics of climate changes, *Rev. Geophys.*, *48*, RG3001, doi:10.1029/2009RG000302.
- Schneider, T., T. Bischoff, and G. H. Haug (2014), Migrations and dynamics of the intertropical convergence zone, *Nature*, *513*, 45–53.
- Seidel, D. J., Q. Fu, W. J. Randel, and T. J. Reichler (2008), Widening of the tropical belt in a changing climate, *Nat. Geosci.*, *1*, 21–24.
- Sobel, A. H., and J. D. Neelin (2006), The boundary layer contribution to intertropical convergence zones in the quasi-equilibrium tropical circulation model framework, *Theor. Comput. Fluid Dyn.*, *20*, 323–350.
- Taylor, K. E., R. J. Stouffer, and G. A. Meehl (2012), An overview of CMIP5 and the experiment design, *Bull. Am. Meteorol. Soc.*, *93*, 485–498.
- Vecchi, G. A., and B. J. Soden (2007), Global warming and the weakening of the tropical circulation, *J. Clim.*, *20*, 4316–4340.
- Voigt, A., and T. A. Shaw (2015), Circulation response to warming shaped by radiative changes of clouds and water vapour, *Nat. Geosci.*, *8*, 102–106.
- Waugh, D. W., C. I. Garfinkel, and L. M. Polvani (2015), Drivers of the recent tropical expansion in the Southern Hemisphere: Changing SSTs or ozone depletion?, *J. Clim.*, *28*, 6581–6586.
- Wodzicki, K. R., and A. D. Rapp (2016), Long-term characterization of the Pacific ITCZ using TRMM, GPCP, and ERA-Interim, *J. Geophys. Res. Atmos.*, *121*, 3153–3170, doi:10.1002/2015JD024458.